LOI Progress Report

– First beam test in April 2011 –

May 11, 2011

1. Introduction

First beam test with LOI, located at SP6, was performed in April 17, 2011 at 2.1×10^{13} protons per pulse (ppp) (fig. 1), which corresponds to the circulating beam current of 2.3 ~ 5.2Amp. The LOI was proven to be stable under such a high intensity beam, and the experimental results were encouraging. The output impedance of LOI was derived from the beam induced voltage across the cavity gap, resulting in 34.3ohm at 3.4MHz, which agrees well with the measurement by the network analyser in 2009. Although the LOI gap voltage was low compared to the original second harmonic RF (2RF) system, acceleration test could have demonstrated the possible usefulness of the LOI for higher RF trapping efficiency at the injection stage. At the end of experiment, ferrite bias current optimization was investigated without beam from view point of the minimum triode current.

In the following sections are reported, output impedance in section 2, acceleration test in section 3, bias current optimization in section 4, faults and remedies in section 5, and discussions & conclusions in section 6.

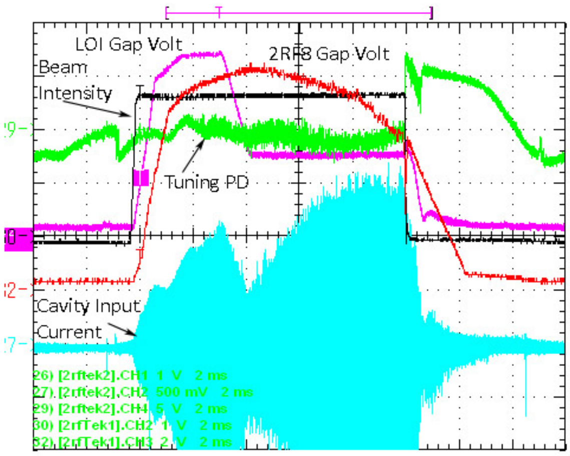

Fig. 1: First acceleration test with LOI and 2RF8 system at beam intensity of 2.1×10^{13}ppp, where peak voltages are 4kV and 10kV, respectively. Tuning phase detection (PD) and cavity input current are in 50° and 10A/div, respectively.

2. Output impedance

Beam induced voltage was measured with RF on for all the fundamental and 2RF8 systems, while no RF for the other 2RF systems: LOI and 2RF5 cavities are fed with a dc bias current and the 2RF4 cavity is kept in “off-tune” mode. The dc bias current was set so that the cavity will resonate at 3.4MHz at 2.16msec after field minimum: bias current is 508A for 2RF5 and 495A for LOI cavity. The reason of this frequency selection is to exclude the effect of other harmonics which ranges from 1.3~3.1MHz for fundamental, and 3.9~9.3MHz for third harmonic components. Fig.2 shows the beam induced voltage in each cavity. The voltage shows a sharp peak at 2.16msec for the 2RF5 cavity where the driver amplifier (Burle 4648 tetrode) is switched off. Such resonant structures cannot be seen for other systems. The voltages at 2.16msec are 6.24kV, 156V and 600V for 2RF5, LOI and 2RF4, respectively.

The 2RF cavity comprises two half-cavities coupled with a bias winding (fig. 3). The beam induced voltage at resonance is then given by,

$$V_b = 2I_b \times (R // R // Z_{out}),$$

where I_b is the beam current passing through each half-cavity gap, R the shunt impedance of half-cavity and Z_{out} the output impedance of the driver system. For the 2RF5 cavity, $Z_{out} >> R$. The induced voltage is then approximated by,

$$V_b \cong 2I_b \times R/2 \qquad \text{for 2RF5 cavity.} \qquad (1)$$

For the LOI, Z_{out} is much lower than R. Then,

$$V_b \cong 2I_b \times Z_{out} \qquad \text{for LOI + 2RF6 cavity.} \qquad (2)$$

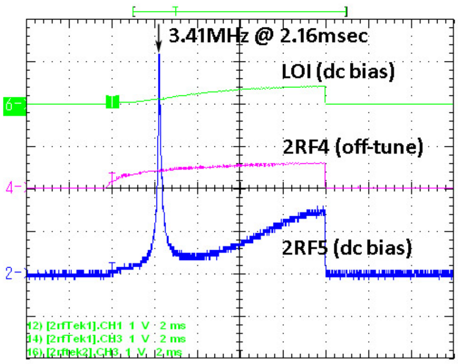

Fig. 2: Beam induced voltage for LOI, 2RF4 and 2RF5 cavities. Dc bias is set for the cavity to resonated at 3.4MHz for LOI and 2RF5.

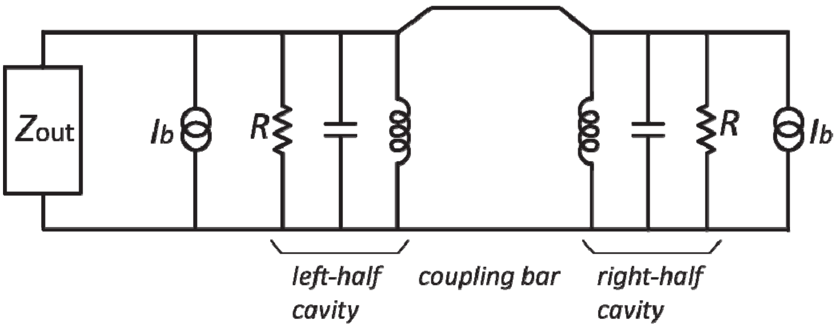

Fig. 3: Equivalent circuit of beam-cavity interaction for two-gap system.

Fig. 4 shows the beam bunch shape at 2.10msec, which is given by the sum signal of vertical electrodes of the R6BM1 beam position monitor. The conditions for 2RF systems are that 2RF8 is on with RF, LOI is on with dc bias and 2RF4 and 5 are in off-tune mode. (*Experimental condition was not the same with that for induced voltage measurement*?!). The bunch shape can be expanded as a Fourier series as

$$BS(t) = a + \sum_{k=1}^{n} c_k \sin(2\pi k f_0 t + \theta_k), \qquad (3)$$

where f_0 is the fundamental frequency, 1.6854MHz, n = 15, and c_k and θ_k the parameters to be fitted. The fitted curve is shown with red-line in fig. 4. The beam current in the ring is related to eq.(3) as,

$$I(t) = I_{conv}(BS(t) - offset),$$

where I_{conv} is the normalization factor and offset the pedestal level of the measured data (-74.19mV). I_{conv} can be obtained from the relation,

$$\oint_{revolution} I(t)dt = \Sigma,$$

where Σ is the total charge in the ring: $\Sigma = 2.06\times10^{13}\times1.60\times10^{-19}$ C. Then, $I_{conv} = 38.5$. The coefficients in eq. (3) and absolute harmonic currents ($I_{conv}\times c_k$) are listed in table 1.

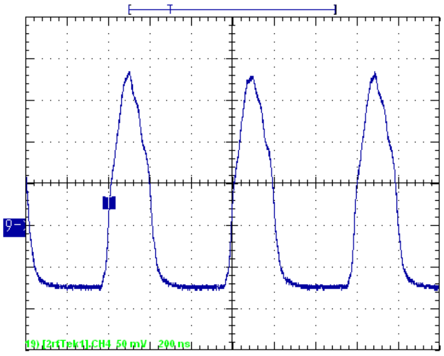

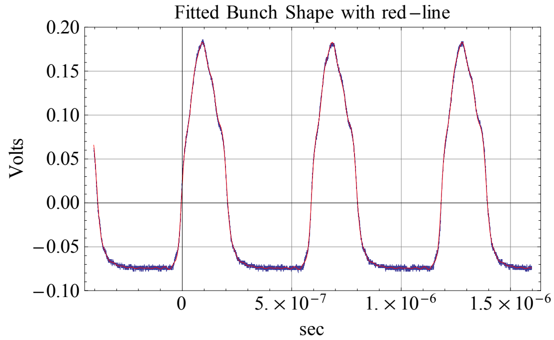

Fig. 4: Beam bunch shape at 2.10msec after field minimum. (Left) measured one as a sum signal of the beam position monitor (0.2usec/div and 50mV/div). (Right) fitted signal with Fourier series in red-line.

Table 1: Beam current component at 2.10msec.

k	c_k	$\lvert c_k \times I_{conv}\rvert$ [Amp]
1	0.116	4.48
2	0.058	2.23
3	-0.012	0.45
4	0.010	0.37
5	-0.006	0.21
6	0.003	0.13
7	0.006	0.22
8	0.002	0.08
9	0.002	0.09
10	0.003	0.12

Using the 2RF current component ($k = 2$) in table 1 and eq. (2), the LOI output impedance is derived to be

$Z_{out} = 35.0$ohm for LOI.

34.3ohm. In fig. 5, this value is compared with the measurement in 2009 [1]. Good agreement is obtained. Similarly, the cavity shunt impedance is obtained with eq. (1) as

$R/2 = 1.37$kohm for 2RF5 cavity. (4)

If the shunt impedances of 2RF5 and 2RF6 cavities are the same, impedance reduction by using the LOI is 1/40.

It must be reminded, however, that the shunt impedance in eq. (4) is different by a factor of three from those obtained in ref. 2 [2]. The reason is not clear at the moment, but probably it should be investigated through the bias optimization process.

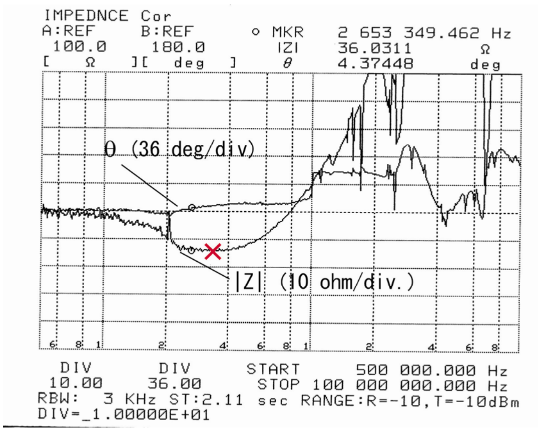

Fig. 5: Comparison of LOI output impedance (Z_{out}) at 3.4MHz. Impedance curve (|Z|) is obtained by the measurement with network analyser [1], where the red-cross (35.0ohm) is in this experiment.

3. Acceleration test

LOI cavity lock to the reference fundamental system was enabled before the acceleration test. In order to compensate for the different configurations between the original 2RF6 and the LOI HPDs, an extra inversion was introduced in the CAV-LOCK unit (fig. 6). In the figure, "LOI Cavity Lock" denotes the phase error between LOI and reference fundamental RF waveform, and "LOI Tuning phase detection (PD)" the phase difference between gap and grid voltages. The LOI gap voltage was then gradually increased, while the waveform was also changed from that seen in fig. 6 to that in fig. 1.

During the acceleration test, slight increase of injection efficiency was observed in table 2, where 2RF4 and 5 are in off-tune mode. Also, it was witnessed that gapvolt oscillation at 2RF8, which is usually seen at later acceleration stage, was damped significantly.

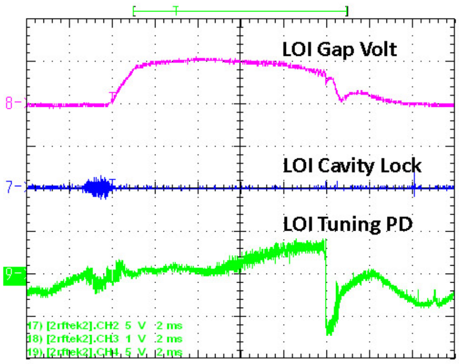

Fig. 6: Setup for acceleration test. From top , LOI gap voltage (1.2kV/div), cavity lock (50°/div) and tuning PD (50°/div).

Table 2: ISIS beam intensity with and without LOI. In the third column, LOI and 2RF8 voltages are 4kV and 10kV peak, respectively (fig. 1).

[10^{13}ppp]	LOI=OFF, 2RF8=ON	LOI=ON, 2RF8=ON
Injected	2.24	2.23
Accelerated	2.07	2.11
On target	2.00	2.01

4. Bias current optimization

The cavity bias current can be controlled by adding the "cavity tune phase demand" to the phase detection signal to produce the "bias demand" at the CAV-TUNE module (fig. 7). In this experiment, the current waveform of the buck regulator (BR) output is always monitored. The bias current is then controlled so as to decrease the increment of the BR current as low as possible when the cavity gap voltage is increased. The cavity input current showed similar tendency when the triode current is decreased (fig. 8).

The optimization process was not completed due to time shortage (as before!). Especially, tuning is not good at the later stage of acceleration, because the cavity input current is very high although the cavity gap voltage is rather low. However, new record was obtained in this optimization process for the LOI gap voltage with 5.3kV peak at the same waveform seen in fig. 1.

Hereafter, optimization will be focussed upon investigating the minimum BR current and the phase relations between cavity gap and grid voltages, and/or between cavity gap voltage and grid input current [3].

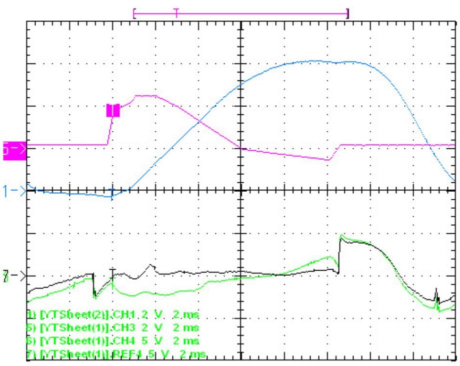

Fig. 7: From top, cavity tune phase demand (pink, 2V/div), bias demand (blue, 2V/div), tuning PD before (black, 50°/div) and after adding phase demand (green, 50°/div).

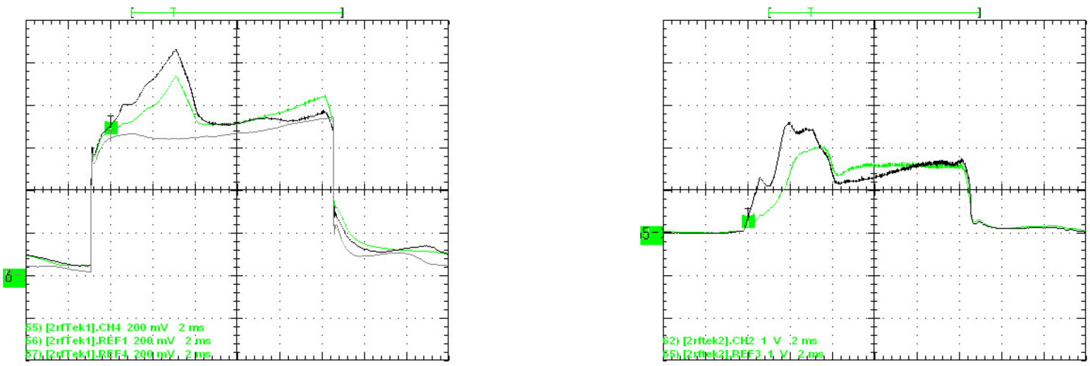

Fig. 8: (Left) Buck regulator output current (5A/div) without RF (grey), with RF but before (black) and after (green) cavity tune phase demand. (Right) Cavity input current (20A/div) before (black) and after (green) cavity tune phase demand. All signals are in 32× average mode. *Note*: *calibration of 25A/V is used for BR output current instead of 35A/V so far*.

5. Faults and remedies

<u>Grid switcher</u>

At the end of this experiment, the IGBT switch (IRG4PH20K) was failed again due to short between gate and emitter. The 15V-zener diode was then installed between them as a surge absorber. However, chattering occurred as shown in fig. 9. The situation became worse when the diode was replaced with higher voltage zener diode (18V). Finally, chattering was ceased when bi-directional diode configuration was applied (fig. 10).

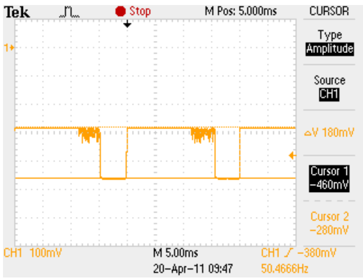

Fig. 9: Chattering of the grid switcher output. It appeared when zener diode was inserted between gate and collector of the IGBT switch (see fig. 10). This was stopped by using bi-directional diode configuration.

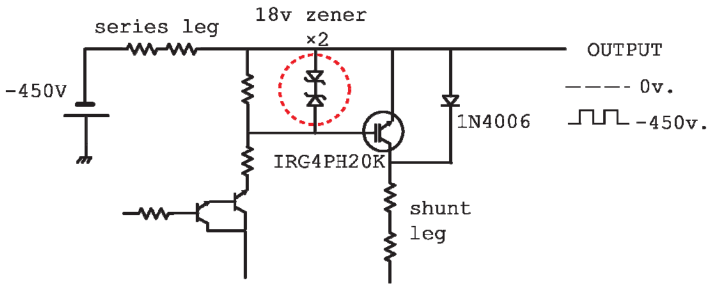

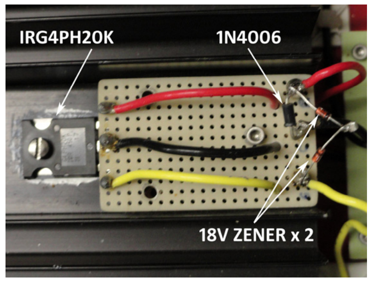

Fig. 10: Bi-directional diode connection between gate and emitter at the grid switcher output stage.

6. Discussions and conclusions

First beam test with LOI was carried out in April 17, 2011, and the results were very encouraging. For further study on the application of LOI, the bias current optimization and sufficient water supply to all the 2RF's will be the important issues. As for bias optimization, it is essential to solve the waveform distortion of the grid voltage due to sub-harmonic content in the RF law signal [4]. Waveform distortion causes an error in the phase detection. However, to make the matters complicated, it is thought that waveform distortion is changeable depending upon the degree of cavity tuning.

References:

[1] LOI Progress Report LOI-6, http://www-accps.kek.jp/Low-Impedance_Cavity/LOI-6.pdf
[2] LOI Progress Report LOI-2,
http://www-accps.kek.jp/Low-Impedance_Cavity/LOI02.August.05.pdf
[3] LOI Progress Report LOI-10, To be uploaded.
[4] LOI Progress Report LOI-8, http://www-accps.kek.jp/Low-Impedance_Cavity/LOI-8.pdf